Open Access

Journal of Energy and Power Technology

LIDSEN Publishing Inc.

Original Research

Surface Treatment of Flexible Barrier Film for Improved Stability of Organic Photovoltaic Mini Modules

Clara L. e Silva [†], Bárbara H.S. Miranda [†], Maria L. Vilela, Jair F. Rodrigues, Thainá G. Cunha, Jhonatan A. Dias, Gabriela A. Soares, Vinicius Freitas, Rodrigo de Q. Vilaça, Luana Wouk, Diego Bagnis [*]

CSEM Brasil, 2000 Sete, Horto Florestal, 31035-536, Belo Horizonte, Minas Gerais, Brazil; E-Mails: clara.lisa.silva@gmail.com; barbara.miranda@csembrasil.com.br; mluizavilela@csembrasil.com.br; jair.rodrigues@csembrasil.com.br; thaina.cunha@csembrasil.com.br; jhondiasgomes@gmail.com; gabriela.amorim@csembrasil.com.br; viniciusvaledefreitas@gmail.com; rodrigo.vilaca@csembrasil.com.br; luanawouk@gmail.com; diego.bagnis@csembrasil.com.br

† These authors contributed equally to this work.

* **Correspondence:** Diego Bagnis; E-Mail: diego.bagnis@csembrasil.com.br

Academic Editor: Zhao Yang Dong

Special Issue: Wind and Solar Energy Conversion System

Journal of Energy and Power Technology
2022, volume 4, issue 3
doi:10.21926/jept.2203023

Received: March 07, 2022
Accepted: June 19, 2022
Published: July 04, 2022

Abstract

The lifetime and stability of organic photovoltaics (OPVs) are the key factors that influence the technology used to scale up and commercialize OPVs. High-performing and reliable devices are used to fabricate the devices of choice. Materials and methods that can be used to prevent the degradation of organic materials, enabling better OPV applications, are being increasingly researched in recent years. Herein, we present the surface modification process of a commercial, flexible barrier film based on polyethylene terephthalate (PET). A sol-gel deposition method was used to modify the surface. Two scalable coating techniques, spray- and bar-coating, were investigated as the processing methods. Treated films were optically, morphologically, and topologically characterized. The modification of the barrier film surface increased the surface hydrophobicity of the bar-coated and spray-coated treated films. This

was validated by the contact angle measurements. OPV roll-to-roll (R2R) mini-modules with 4.2% power conversion efficiency were fabricated and encapsulated with the treated films. The lifetime and stability were assessed by conducting accelerated aging tests based on the ISOS-D-3 protocol. The spray-coating technique provided a more stable layer than the bar-coating technique, and the lifetime of the OPV modules encapsulated in spray-coated treated barrier films was increased. Surface modification has been demonstrated to be a promising approach for not only improving the barrier film properties (resulting in the improved lifetimes of the modules) but also reducing the extents of reflectance losses in the OPV modules post encapsulation.

Keywords
Flexible barrier films encapsulation; lifetime; organic photovoltaic (OPV); spray-coating; bar-coating; surface treatment

1. Introduction

The development of renewable energy resources, especially photovoltaics, is attracting extensive attention as there has been a rapid increase in global energy consumption in recent years [1, 2]. Organic photovoltaics (OPVs) represent an attractive class of photovoltaic materials that are better than traditional silicon-based and inorganic thin-film solar cells [3]. These are cost-effective materials that can be processed at low temperatures following the energy-saving roll-to-roll (R2R) processing method [4]. The OPVs are lightweight and flexible and exhibit free-shape properties. Thus, they can be effectively used for the fabrication of integrated PVs. These can be used as building-integrated photovoltaics (BIPV) and building applied photovoltaics (BAPV) [5, 6].

Photovoltaics, especially when used outdoors, are subjected to various stressors that result in the degradation of organic materials. Ultraviolet (UV) radiation, temperature, and moisture (or, more generally, oxygen) function as stressors [7-10]. These stressors can compromise the lifetime of the OPVs, which is dependent on the effective working conditions of the active materials in the device [11, 12]. The maximum extent of degradation is caused by external elements, and an optimal solution can be prepared to protect the devices from such environments. Hence, the process of encapsulation using ultra-high barrier materials has been studied [13-15]. To increase the potential industrial applications for such devices, the process of encapsulation is preferably conducted using flexible barrier films. Inorganic thin-film materials offer a high barrier toward moisture permeation. However, these materials are brittle and not crack resistant. Organic polymer-based encapsulants cannot effectively hinder the entry of oxygen and moisture. However, these materials are flexible, can be easily processed, and exhibit good conformability. Hence, a combination of both organic and inorganic materials meets the requirements of flexibility, and these materials can be used to generate a high gas and oxygen barrier [13]. Numerous approaches for OPV device encapsulation using single-layered/curing/composite/multilayered films have been studied [16-19]. However, commercially available barrier layers should be improved further to offer the required protection to the devices to increase their long-term performance [20], the properties of which are better than those of the traditional photovoltaic devices

A beneficial and cost-effective method to improve the barrier properties of the materials involves surface treating the barrier films [21]. A promising approach involves developing hydrophobic functional coatings that can be used to provide long-term protection and develop easy-to-clean surfaces. The use of this method can positively influence the appearance, operation conditions, and lifetime of the panels [22]. Organic–inorganic hybrid materials such as silica sol-gel coatings are particularly effective [21]. Surface treatment methods can help improve the optical properties of the barrier film. During the operation of the solar cells, a large amount of energy is lost due to surface reflection [23]. Functional coatings that can be used to realize low-reflection and high-transmittance of light may significantly affect the performance of the solar cells [24-26]. Under adequate treatment conditions, a surface can efficiently regulate the amount of solar radiation passing through it [26]. Various treatment methods can be potentially used to modulate the wavelengths that pass through the device. The barrier can function as a filter that helps remove the most harmful parts of the solar spectrum [8].

In this work, a surface treatment method for treating commercial flexible barrier films was developed to investigate the influence of the films on the performance and lifetimes of the OPV devices. A commercial sol–gel solution was deposited onto flexible barrier films formed of polyethylene terephthalate (PET) following the spray-and bar-coating methods. Optical microscopy, contact angle measurement, atomic force microscopy (AFM), and ultraviolet-visible spectroscopy (UV-vis) techniques were used to examine the coating properties. The OPV mini-modules processed following the R2R slot-die coating method were fabricated and encapsulated within the treated barrier films. The degradation of the systems under accelerated aging conditions followed the ISOS-D-3 protocol [27, 28].

2. Materials and Methods

2.1 Surface Treatment of Flexible Barrier Films following the Spray-Coating Technique

Cleanrise (22%, w/w, solution, see Table S5 and Table S6) purchased from Polyrise Innovative Coating Technology (France) was coated on top of a 61 μm-thick commercial barrier film (15 cm × 20 cm) obtained from Mitsubishi Plastics INC. The barrier film consists of a multilayer of oxides sandwiched between flexible substrates based on PET. The water vapor transmission rate (WVTR) was 4.8×10^{-3} g/cm^2/day, and 88.5% of transmittance was achieved (cut-off: 380 nm; <6.0% transmittance). An airbrush (SH40305-AU; nozzle diameter: 0.5 mm) was used for the studies, and the solution droplets were deposited onto the substrates using a flow of pressurized nitrogen gas (33 ±4 PSI). A distance of 10 cm was maintained between the nozzle and the sample. An internally engineered customized system holder (Figure S1a) was used during the process. The solution and the substrate were stored at room temperature during the process of deposition. The process of deposition was followed by a curing step that was conducted at 120°C for 10 min on a hot plate (Thermo Scientific, Cimarec). Two different volumes and speed combinations were investigated to form a 1.0 μm-thick dried layer. The solution (2.0 mL) was deposited at a rate of 1.5 s/run, and 1.0 mL of the solution was deposited at 0.8 s/run. The spray-coating process was also studied by depositing 1.0 mL of the solution by conducting 2, 6, and 8 runs.

2.2 Surface Treatment of the Flexible Barrier Film following the Bar-Coating Process

The bar-coating process was conducted using Blade Coater equipment (Erichsen, COATMASTER 510) and an internally fabricated copper wired bar (diameter: 10.5 mm) (Figure S1b). Cleanrise (580 µL; 22%, w/w, see Table S5 and Table S6) and a bar gap of 600 µm were used to conduct the process. Various bar-coating speeds (5.0 mm/s, 10 mm/s, 20 mm/s, 30 mm/s, and 40 mm/s) were tested to determine the optimal conditions. The solution was coated on top of the barrier film at room temperature under the conditions used to execute the spray-coating process. The final samples were obtained following a curing step conducted at 120°C for 30 min. The curing step was conducted inside an oven (Thermo Scientific, model OMH190-S).

2.3 OPV Mini Modules: Fabrication and Encapsulation

Layers of OPV minimodules were slot-die coated using a single station R2R lab machine (Smart Coater SC09, Coatema Coating Machinery GmbH). An inverted structure was fabricated using a pre-patterned PET substrate covered with a multilayered sputtered indium tin oxide (ITO)/silver/ITO (IMI). This was used as the bottom electrode (10 Ω/sq, 83.6% transmittance at 526 nm, Oike&Co. Ltd., Japan). An amine-based electron transport layer (ETL) and an active layer (AL) consisting of a low band-gap copolymer (1.67 eV) and a PC60BM-derivative acceptor dissolved in o-xylene were prepared. A commercial highly conductive PEDOT:PSS system with a 400–450 nm-thick coat was used as HTL. Finally, mini-modules (active area: 21.6 cm^2) consisting of 6 individual series-connected cells were developed using a flatbed screen printing system and a silver paste (Ag content: 80%). A photograph of the module is shown in Figure 1. To prevent environmental degradation, the modules were encapsulated in the air under environmental laboratory conditions (relative humidity: <50%) using treated (following spray-and bar-coating methods) and non-treated barrier films. An epoxy-based UV-curable adhesive with additional barrier properties was used as an encapsulant. The bar-coating method was used to directly coat the material on the barrier films. The resin was irradiated using a 395 nm-peak UV lamp to initialize the process of curing. Subsequently, the materials were thermally treated at 85°C for 4 h.

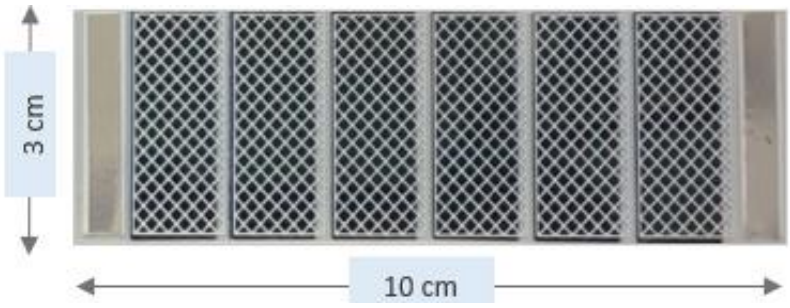

Figure 1 Photograph of the 6 series-cell equipped OPV mini-module characterized by an active surface of 21.6 cm^2.

2.4 Characterization of the Barrier Films and Devices

The quality of the OPV-treated barrier films was evaluated using an optical microscope (Leica, model DFC295) at 50× magnification. The thicknesses of the coated layers were assessed using a profilometer (Bruker, DektakXT Stylus). The water contact angle was measured using (0.5 µL; water

droplet) a contact angle equipment from Ossila. Optical transmittances of the neat film and the best-treatment conditions were determined using a UV-vis spectrometer (Shimadzu, model UV-2600). The morphology was studied using the AFM technique. The topographic images were obtained under the non-contact mode (Asylum Research, model Cypher ES and Park XE7).

The current density–voltage (J–V) curves corresponding to the OPV mini-modules were recorded before and after encapsulation under 1-Sun illumination conditions using a Class AAA solar simulator (Wacom WXS-156S-10) equipped with a Xenon lamp. The AM 1.5G spectrum was recorded. The external quantum efficiency (EQE) and internal quantum efficiency (IQE) of the devices were measured using a PTS-2-QE Quantum Efficiency/IPCE System from Sciencetech. Lastly, an accelerated degradation test was carried out for devices encapsulated with treated and non-treated barrier films following the ISOS-D-3 protocol. The test was performed in a climate chamber (SPX, model CEO932–4) at 65°C (relative humidity: 85%). The test was completed when the relative efficiency of the mini-modules dropped to 50% of the initial efficiency. Six modules of each condition were analyzed to ensure repeatability.

3. Results

3.1 Spray-Coated Films

The optical microscopy images recorded for the spray-coated samples revealed that the film formation process involved the deposition of solution droplets onto the substrate, as shown in Figure 2a and Figure 2b. The uniformity of the solution was influenced by the speed of the process. A highly homogenous film was formed when the films were processed at 0.8 s/run. The appearance of the film was negatively affected by the irregularity in the speed of the spray-coating process. The treated films became hazier than the untreated films, and the haziness could be observed with naked eyes (Figure 2c). Additionally, the thickness varied significantly because of the inhomogeneity of the surface. The average film thickness assessed by profilometry was 1.4±0.8 µm. The best processing conditions for the spray-coating method are summarized in Table S1.

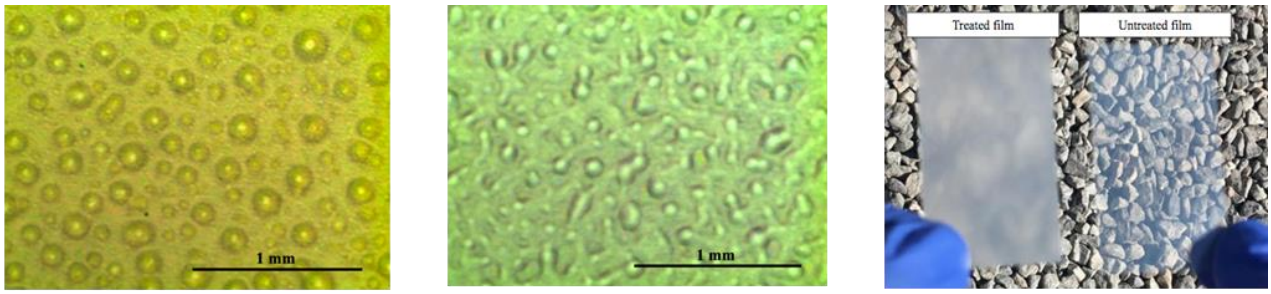

(a) (b) (c)

Figure 2 Optical microscopy images (50× magnification) of (a) samples processed at 1.5 s/run and (b) 0.8 s/run. (c) Comparison of the appearance of the non-treated film with the film treated following the spray-coating method.

3.2 Bar-Coated Films

As shown in Figure 3, the film formed following the bar-coating method was more homogeneous than the film formed following the spray-coating method. Analysis of the untreated standard barrier

film (analyzed using the optical microscopy technique) revealed the presence of surface heterogeneities. These can potentially result in differences in the thicknesses of the films deposited onto the surfaces following the bar-coating method. Overall, the most homogeneous films were prepared when the speed was 5.0 mm/s. The degree of haziness observed did not significantly change in the presence of heterogeneities (Figure 3c).

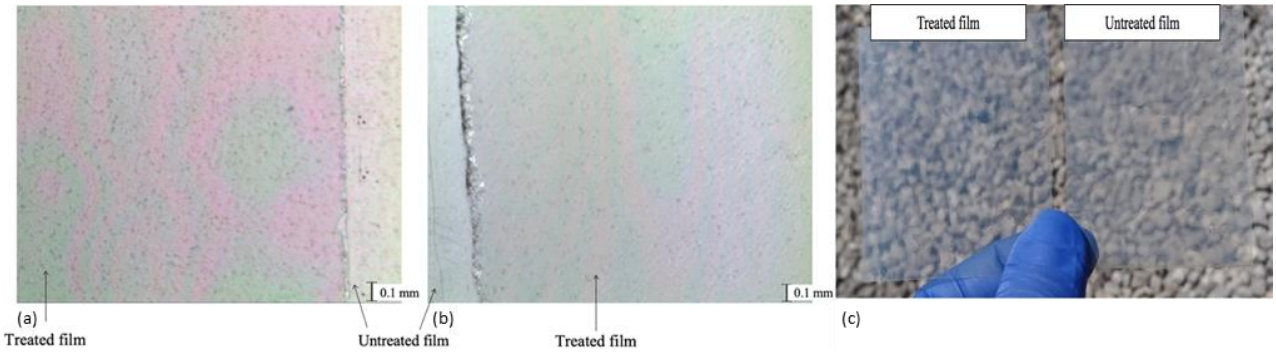

Figure 3 Optical microscopy images (50× magnification) of (a) samples processed following the bar-coating method at the speed of 5 mm/s and (b) 20 mm/s. (c) Comparison of the appearance of the non-treated film with the appearance of the film treated following the bar-coating method.

The thickness of the dried film depends on the speed of the bar-coating process, as illustrated in Figure 4. This is in accordance with previously reported results [29]. The thickness of the dried film was 1.43 ±0.13 µm and 2.69 ±0.49 µm when the processing speeds were 5.0 mm/s and 20 mm/s, respectively. It was also noted that the thickness limit was 3.81±0.43 µm. The maximum thickness could be achieved under defined process parameters. Significant differences in the thicknesses were not observed when the films were processed at 30 mm/s and 40 mm/s (Figure 4). The best processing conditions for the bar-coating method are summarized in Table S2.

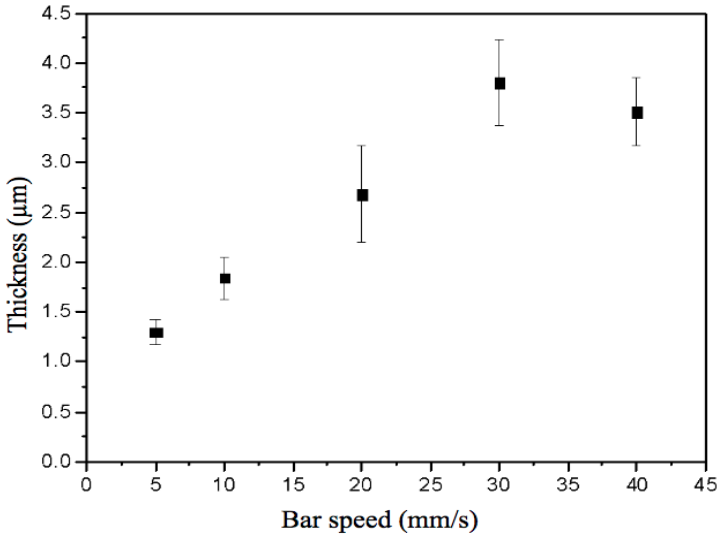

Figure 4 Thickness of the film deposited following the bar-coating method as a function of the bar speed.

3.3 Characterization of the Barrier Films and Devices

The hydrophobicity of the treated surface was investigated using the water contact angle method. Analysis of the bar-coated surfaces (Figure 5) revealed that the contact angle increased by 40% after coating, demonstrating the hydrophobic characteristics of the surface. The same contact angle was recorded when the spray-and bar-coating methods were used (Figure S2). It is well-known that the hydrophobicity of a surface is governed by surface chemistry. Surfaces characterized by a high-water contact angle exhibit high water repellent properties [30]. An increase in the contact angle indicates that the free surface energy decreases upon the application of the film. Low surface energy is desired for a barrier film for OPV encapsulation, especially under outdoor conditions [31]. Therefore, a high contact angle could potentially help reduce the extent of water penetration (into the barrier). The OPV stack degradation mechanisms are mitigated when chemical reactions occur with water and oxygen in the atmosphere or ambient environment [7, 14].

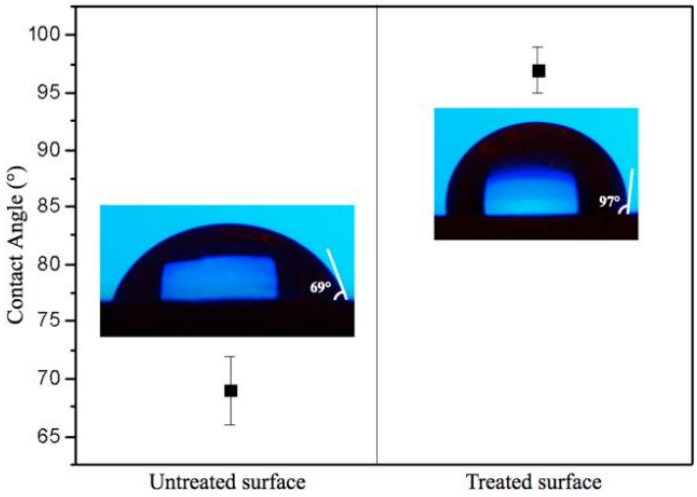

Figure 5 Contact angles determined for water droplets on top of treated (bar-coat treatment process) and non-treated barrier films.

The UV-vis transmittances corresponding to the non-treated and treated films are shown in Figure 6. The degree of transmission recorded for the film treated following the spray coating method was lower than the degree of transmittance recorded for the non-treated film. The results reflected the fact that the haziness of the samples increased post treatment. Conversely, an increase in transmittance was observed for the films treated following the bar-coating method. A comparison of the transmittance values recorded at 700 nm is shown in Table 1. The absorption spectral profiles recorded for the OPV active layer, the reference film, and the films bar-coated at 5 mm/s are illustrated in Figure 6b.

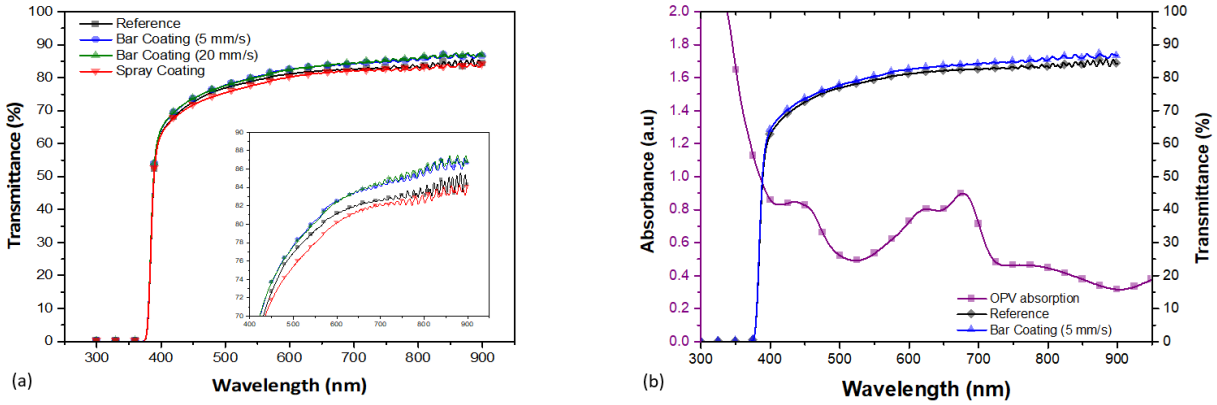

Figure 6 (a) UV-vis transmittance recorded for non-treated and treated surfaces (treatment methods: spray-coating and bar-coating; speed: 5 mm/s and 20 mm/s) and (b) comparison of the profiles recorded for the OPV active layer, reference layer, and bar-coated (5 mm/s) films.

Table 1 Comparison between the transmittances recorded under varying conditions at 700 nm.

	Transmittance (%)	**Change with respect to the reference**
Reference	82.59	-
Bar-coating (5 mm/s)	84.14	+1.88%
Bar-coating (20 mm/s)	84.45	+2.25%
Spray-coating	82.14	-0.53%

Analysis of the AFM topography of the non-treated (Figure 7a) and treated barriers bar-coated at 5.0 mm/s (Figure 7b) revealed that the surface morphology was modified by the sol–gel coat. The surface roughness reduced significantly under these conditions. The root mean square (RMS) recorded for the barrier film was 8.9 nm, whereas the RMS for the treated barrier was 0.9 nm. The decrease in roughness suggests that the sol–gel layer covered the substrate well, forming a smooth fiber-like structure. The change was corroborated by the changes observed in Figure 6a. Analysis of the topography of the sample coated at the rate of 20 mm/s reveals the formation of a smooth fiber-like structure (RMS: 1.9 nm). This sample was smoother than the sample coated at the rate of 5.0 mm/s. A valley–hill pattern, attributable to the uniformity of the coat, was observed. Analysis of the phase image reveals the presence of an agglomerate, suggesting that the surface processed at 20 mm/s was inhomogeneous. The inhomogeneities could be attributed to the high coating speed [29].

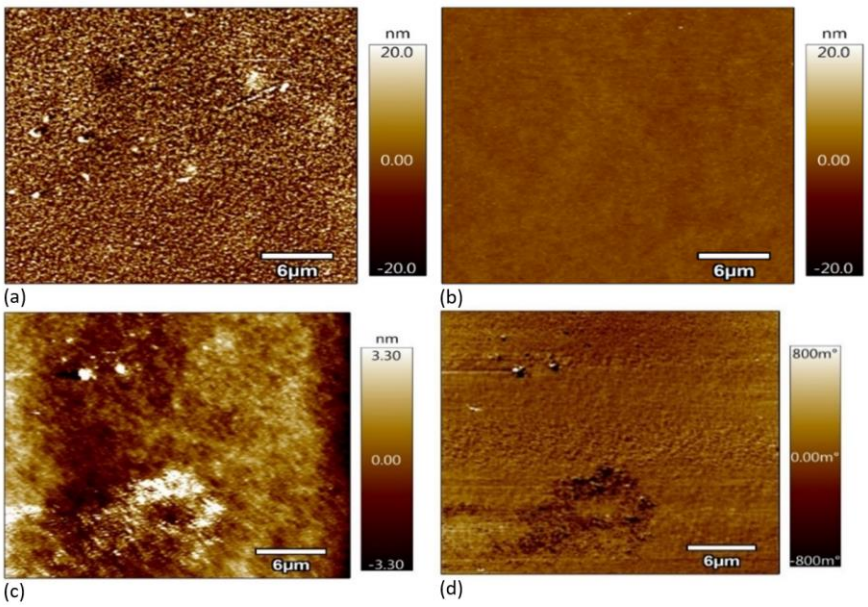

Figure 7 AFM topography of (a) non-treated film, (b) bar-coated barrier film coated at the speed of 5 mm/s, and (c) bar-coated barrier film coated at the speed of 20 mm/s. (d) AFM phase image of the bar-coated film treated at the speed of 20 mm/s.

The AFM topography (Figure 8) of aged spray-coated films revealed a fiber-like structure that was similar to the structure of blade-coated samples. A decrease in the surface roughness of the barrier film following the deposition of the film was also observed. The RMS value was recorded to be 2.4 nm. It was inferred that the surface roughness of the spray-coated films was slightly higher than the surface roughness of the blade-coated films. The results agree with the results obtained using the optical microscopy technique and the data obtained using the profilometer. It was also revealed that the roughness of the treated films was lower than the roughness of the untreated films. The results suggested the presence of surface irregularities, confirming previous observations. AFM images of the bar-coated samples recorded within the same time period are presented in Figure S3.

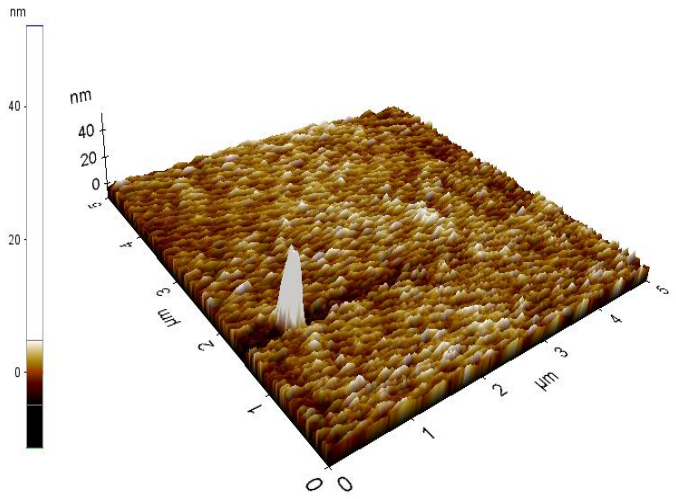

Figure 8 3D AFM topography of aged spray-coated barrier films.

The PV performances of the OPV mini-modules encapsulated with spray-coated films were recorded before and after encapsulation, and the results were compared with the results obtained by analyzing the reference devices. The main PV parameters are presented in Figure 9 and summarized in Table S3. A drop in power conversion efficiency (PCE) was observed after encapsulation for both the reference and spray-coated films. The decrease in the value can be primarily attributed to the high decrease in the open-circuit voltage (VOC, see Figure 9c) and shunt resistance (RSH, Figure S3b). The drop in the VOC and RSH values is related to the pressure and temperature applied during the encapsulation process. A decrease in the values was also observed in other OPV experiments conducted at the CSEM Brasil laboratory.

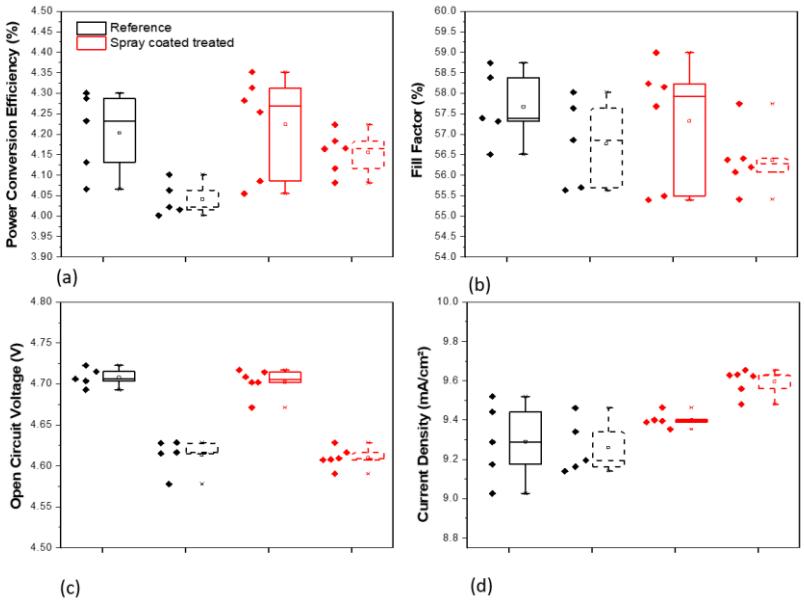

Figure 9 Statistics of photovoltaic parameters. (a) Power conversion efficiency, (b) fill factor, (c) open-circuit voltage, and (d) current density corresponding to the reference and encapsulated mini-modules with spray-coated barrier films. The continuous lines represent the performance before encapsulation, while the dashed lines represent the performance after encapsulation.

The mini-modules encapsulated with the superficially treated barriers following the spray-coating method performed better than the reference devices. A low PCE loss (1.61%; drop in the reference system: 3.87%) was realized. This behavior could be attributed to an increase (by 2.08%) in the short circuit current (JSC) after encapsulation. Statistical differences among the JSC of the modules encapsulated with non-treated films were recorded. The increase in the values can be attributed to the changes in the morphology of the barrier film surface attributable to the process of sol-gel deposition. The degree of reflectance losses realized decreases under these conditions, as shown in Figure 10.

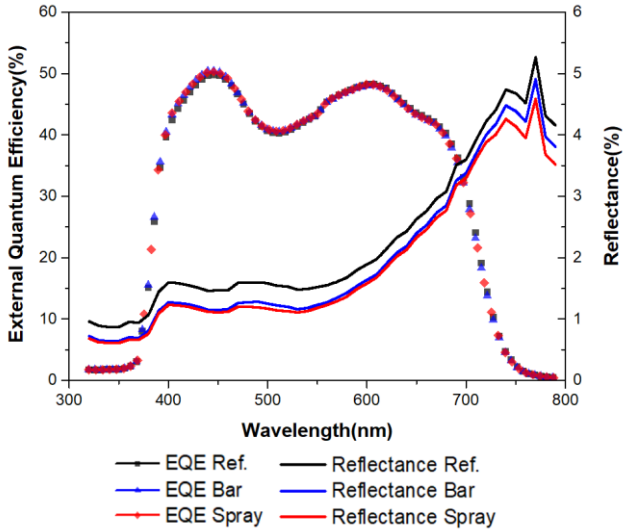

Figure 10 External quantum efficiency recorded for mini-modules encapsulated with treated and untreated films. The bar-coating method was conducted at the rate of 5 mm/s.

The PV performances of the devices encapsulated with the bar-coated films are illustrated in Figure 9 and summarized in Table S4. For the mini-modules encapsulated with spray-coated barriers, the VOC (see Figure 11c) and RSH (see Figure S4b and Figure S5b) parameters decreased under all conditions, resulting in a decrease in the fill factor (FF). The JSC values corresponding to the samples encapsulated with the bar-coated barriers increased under both conditions (2.37% and 20.08% for 5.0 mm/s and 20 mm/s, respectively). The maximum JSC value was recorded for the thickest layer coated at the speed of 20 mm/s. Conversely, the JSC values corresponding to the reference samples decreased by 1.47% post encapsulation. As a result, the photovoltaic performance of the devices post encapsulation improved, as shown in Figure 9a. These changes can be attributed to the increase in the degree of transmittance (Figure 6) and the decrease in the reflectance losses (Figure 10).

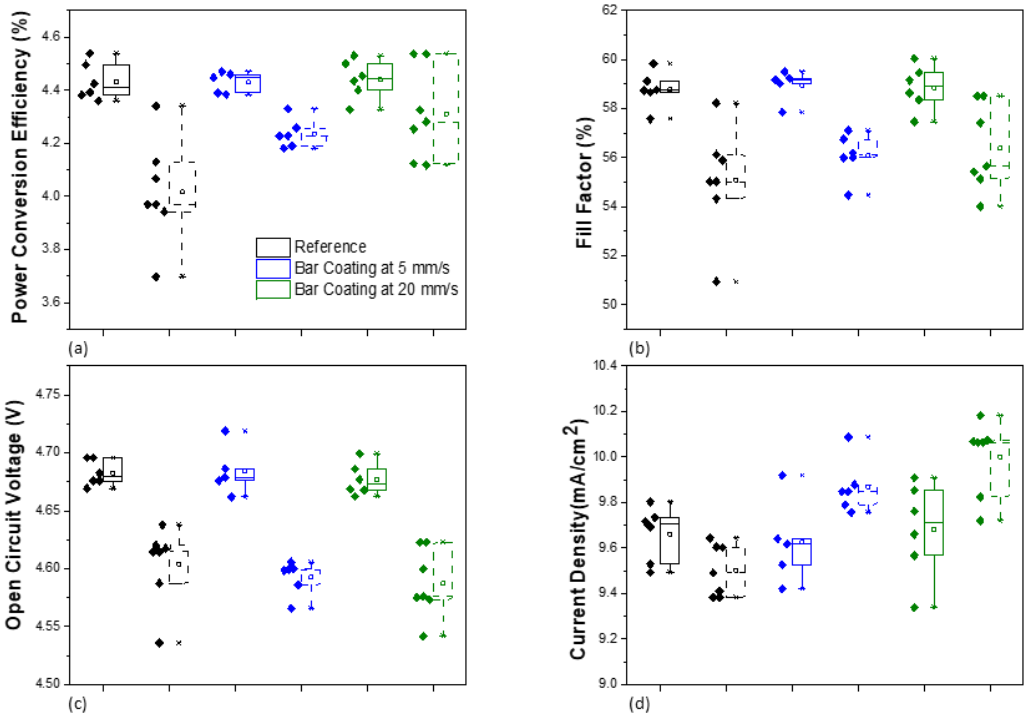

Figure 11 Statistics of photovoltaic parameters. (a) Power conversion efficiency, (b) fill factor, (c) open-circuit voltage, and (d) current density corresponding to the reference and encapsulated mini-modules with bar-coated treated barrier films. The continuous lines represent the performance of the system before encapsulation, while the dashed lines reflect the performance of the system after encapsulation.

Quantum efficiency (QE) quantifies the amount of current that a photovoltaic cell produces when irradiated by photons of a particular wavelength. Two types of QE measurement methods are used for analysis: EQE and IQE. EQE is defined as the ratio of the number of charge carriers collected by the solar cell to the number of incident photons at a given wavelength. It is an important tool to quantify the number of charges collected at the electrode per incident photon of specific energy [32]. On the other hand, IQE takes into account only the absorbed photons, considering only the incident light that reaches the active region [33]. The EQE and the reflectance values corresponding to the reference mini-modules and the systems encapsulated with the treated barriers are illustrated in Figure 10, while the IQE spectrum is shown in Figure S6. The reflectance was lower for the treated samples than the reflectance recorded for the untreated samples, which can explain the increase in the JSC values under all conditions (Figure 9d and Figure 11d). The lowest reflectance values were recorded for the films treated under conditions of spray-coating. Thus, the low reflectance loss incurred by the spray-coated films might compensate for the low transmission efficiency (Figure 6). This can potentially explain the similar behavior of the bar-and spray-coated photovoltaic system.

Figure 12 and Figure 13 show the evolution of the PCE, VOC, FF, and series resistance (RSERIES) of encapsulated modules over time under accelerated degradation conditions. Compared to the reference modules, the PCE of mini-modules encapsulated with spray-coated barrier films showed a smoother decrease (Figure 12a). RSERIES increased significantly with time (Figure 12d), particularly for modules encapsulated with untreated barrier films. Consequently, a significant

decrease in the FF values was recorded for these modules (Figure 12b). This can be attributed to high PCE reduction. The changes in resistance are associated with device interfaces and electrical contacts. These parameters are highly influenced by the water penetration ability. Furthermore, the VOC of the modules encapsulated with non-treated films declined rapidly after 500 h (Figure 12c), which indicates water penetration through the device [10].

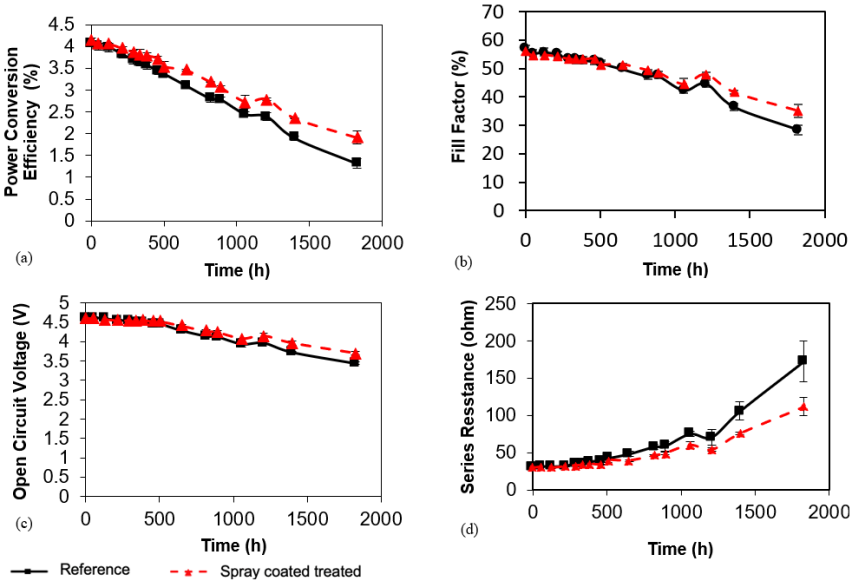

Figure 12 Stability of mini-modules encapsulated with spray-coated barrier films. The devices were tested at 65°C under conditions of 85% relative humidity. (a) Power conversion efficiency, (b) fill factor, (c) open-circuit voltage, and (d) series resistance. Data is normalized to the first value, and the points are connected to reflect the trend.

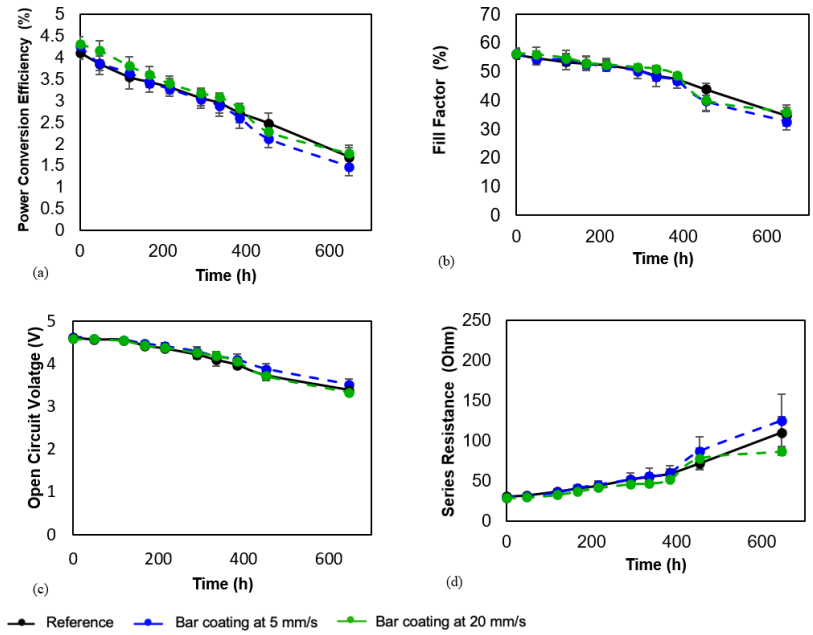

Figure 13 Stability of mini-modules encapsulated with bar-coated barrier films. The devices were tested at 65°C (relative humidity: 85%). (a) Power conversion efficiency, (b) fill factor, (c) open-circuit voltage, and (d) series resistance. Data is normalized to the first value, and points are connected to reflect the trend.

The time taken for the efficiency of the modules encapsulated with spray-coated films to reach 80% (T80) and 50% (T50) of their initial efficiency was 739±63 h and 1681 ±170 h, respectively. Conversely, the reference modules took 573±21 h and 1346±82 h to reflect comparable efficiencies. Thus, under accelerated degradation conditions, the lifetime of the device increased by 28.9% (T80) and 24.8% (T50) post surface treatment.

The process of surface treatment improved the surface hydrophobicity of the bar-coated and spray-coated films, as evidenced by contact angle measurements (Figure 5 and Figure S2). As the ingress of moisture reduces charge carrier mobility [13], the increase in resistance to water penetration indicates a stable PCE. However, the stability of the mini-modules encapsulated with bar-coated barrier films did not improve. The PCE, in this case, was lower than that of the reference (Figure 13a).

Moreover, as there was no improvement in the VOC evolution over time for the bar-coated samples, it suggested that the water resistance of the device did not improve following the modification of the surface following the bar-coating method. These results indicate that the coating process has a significant influence on the adhesion property and durability of the layers deposited on the barrier film. The use of the spray-coating technique resulted in the formation of a stable layer.

4. Conclusions

The barrier film surface modification method helps improve the lifetime of the systems. The hydrophobic characteristics acquired by the surface revealed an improvement in the barrier properties. The OPV mini-modules encapsulated with spray-coated films were more stable under accelerated degradation conditions than the reference systems.

The spray-coating deposition method was more efficient than the bar-coating method in improving the lifetime of the barrier films. Although the photovoltaic performance of the OPV mini-modules encapsulated with the bar-coated films was comparable to the photovoltaic performance of the untreated samples, the stability under accelerated degradation conditions did not show any improvement. This can be potentially attributed to the degree of adherence of the deposited layer. Moreover, spray-coating is a scalable and low-cost process that can be effectively used as an alternative method for large-scale production.

Improvements in the current density attributable to the use of surface treatment methods suggest the important role of light management and interfacial development in the design of organic photovoltaic modules. Results indicated that a decrease in the roughness of the barrier film, revealed by the AFM technique, potentially decreased the degree of light scattering. This allows a larger number of photons to be collected by the OPV active layer. As a result, the degree of reflectance loss decreased significantly. Additionally, an increase in the transmittance level observed for some of the coated films allowed an increase in the amount of light intake. This helped improve the performance of the system.

Author Contributions

Clara L. e Silva: Barrier film surface treatment, OPV mini modules' encapsulation, Photovoltaic measurements, Analysis, Writing-Original Draft & Editing. Bárbara H.S. Miranda: OPV mini modules' fabrication, Supervision, Validation, Analysis, Writing-Review. Maria L. Vilela: OPV mini modules' fabrication. Jair F. Rodrigues: OPV mini modules' fabrication. Thainá G. Cunha: Lifetime

measurements. Jhonatan A. Dias: OPV mini modules' encapsulation. Gabriela A. Soares: Lifetime measurements, Analysis. Vinicius Freitas: Barrier film surface treatment. Rodrigo de Q. Vilaça: Supervision, Validation. Luana Wouk: AFM, EQE, and IQE measurements, Analysis. Diego Bagnis: Supervision, Validation.

Funding

This work was supported by CSEM Brasil.

Competing Interests

The authors have declared that no competing interests exist.

Additional Materials

The following additional materials are uploaded at the page of this paper.

1. Figure S1: (a) Spray-coating equipment. (b) Copper wired bar internally fabricated for the bar-coating process.
2. Table S1: Optimal process conditions for surface treatment using the spray-coating technique.
3. Table S2: Optimal process conditions for surface treatment using the bar-coating technique.
4. Figure S2: Contact angle recorded for water on top of a (a) barrier film treated using the spray-coating technique and a (b) non-treated film.
5. Figure S3: 3D AFM Topography images of aged bar-coated barrier films processed at (a) 5 and (b) 20 mm/s.
6. Table S3: Photovoltaic parameters under 1000 W/m^2 (1-sun) before (BE) and after encapsulation (AE) for devices encapsulated with spray-coated films. The maximum values are presented within parenthesis.
7. Table S4: Photovoltaic parameters under 1000 W/m^2 (1-sun) before (BE) and after encapsulation (AE) for devices encapsulated with bar-coated films. The maximum values are presented within parenthesis.
8. Figure S4: Photovoltaic parameters. (a) Series resistance and (b) shunt resistance corresponding to the reference and the encapsulated mini-modules with spray-coated modified barrier films. The continuous lines represent the performance of the system before encapsulation, while the dashed lines represent the performance of the system after encapsulation.
9. Figure S5: Photovoltaic parameters. (a) Series resistance and (b) shunt resistance corresponding to the reference and encapsulated mini-modules with bar-coated modified barrier films. The continuous lines represent the performance of the system before encapsulation, while the dashed lines represent the performance of the system after encapsulation.
10. Figure S6: Internal quantum efficiency values recorded for mini-modules encapsulated with treated and non-treated films. The bar-coating condition was investigated when the speed of coating was 5 mm/s.
11. Table S5: Details of the thermal cure sol-gel Cleanrise CT1.C171.4 system provided by the supplier (Polyrise).

12. Table S6: Details of the coating and curing processes conducted using Cleanrise CT1.C171.4. The sol–gel coat was designed to impart hydrophobic and oleophobic properties to the system.

References

1. Miranda BHS, Corrêa LQ, Soares GA, Martins JL, Lopes PL, Vilela ML, et al. Efficient fully roll-to-roll coated encapsulated organic solar module for indoor applications. Sol Energy. 2021; 220: 343-353.
2. Inganäs O. Organic photovoltaics over three decades. Adv Mater. 2018; 30: 1800388.
3. Brabec CJ, Sariciftci NS, Hummelen JC. Plastic solar cells. Adv Funtional Mater. 2001; 11: 15-26.
4. Jao MH, Liao HC, Su WF. Achieving a high fill factor for organic solar cells. J Mater Chem. 2016; 4: 5784-5801.
5. Hösel M, Krebs FC. Large-scale roll-to-roll fabrication of organic solar cells for energy production. Copenhagen: Technical University of Denmark; 2013.
6. Etxebarria I, Ajuria J, Pacios R. Solution-processable polymeric solar cells: A review on materials, strategies and cell architectures to overcome 10%. Org Electron. 2015; 19: 34-60.
7. Mateker WR, McGehee MD. Progress in understanding degradation mechanisms and improving stability in organic photovoltaics. Adv Mater. 2017; 29: 1603940.
8. Jørgensen M, Norrman K, Gevorgyan SA, Tromholt T, Andreasen B, Krebs FC. Stability of polymer solar cells. Adv Mater. 2012; 24: 580-612.
9. Corazza M, Krebs FC, Gevorgyan SA. Lifetime of organic photovoltaics: Linking outdoor and indoor tests. Sol Energy Mater Sol Cells. 2015; 143: 467-472.
10. Cheng P, Zhan X. Stability of organic solar cells: Challenges and strategies. Chem Soc Rev. 2016; 45: 2544-2582.
11. Gevorgyan SA, Heckler IM, Bundgaard E, Corazza M, Hösel M, Søndergaard RR, et al. Improving, characterizing and predicting the lifetime of organic photovoltaics. J Phys D. 2017; 50: 103001.
12. Yamilova OR, Martynov IV, Brandvold AS, Klimovich IV, Balzer AH, Akkuratov AV, et al. What is killing organic photovoltaics: Light-induced crosslinking as a general degradation pathway of organic conjugated molecules. Adv Energy Mater. 2020; 10: 1903163.
13. Seethamraju S, Ramamurthy PC, Madras G. Encapsulation for Improving the efficiencies of solar cells. In: Materials and processes for solar fuel production. New York: Springer; 2014. pp.23-40.
14. Lee CY, Tsao CS, Lin HK, Cha HC, Chung TY, Sung YM, et al. Encapsulation improvement and stability of ambient roll-to-roll slot-die-coated organic photovoltaic modules. Sol Energy. 2021; 213: 136-144.
15. Gaddam SK, Pothu R, Boddula R. Advanced polymer encapsulates for photovoltaic devices − A review. J Mater. 2021; 7: 920-928.
16. Ahmad J, Bazaka K, Anderson LJ, White RD, Jacob MV. Materials and methods for encapsulation of OPV: A review. Renew Sustain Energy Rev. 2013; 27: 104-117.
17. Uddin A, Upama MB, Yi H, Duan L. Encapsulation of organic and perovskite solar cells: A review. Coatings. 2019; 9: 65.
18. Kim N, Graham S, Hwang KJ. Enhancement of the barrier performance in organic/inorganic multilayer thin-film structures by annealing of the parylene layer. Mater Res Bull. 2014; 58: 24-27.

19. Hösel M, Søndergaard RR, Jørgensen M, Krebs FC. Comparison of UV-curing, hotmelt, and pressure sensitive adhesive as roll-to-roll encapsulation methods for polymer solar cells. Adv Eng Mater. 2013; 15: 1068-1075.
20. Weerasinghe HC, Vak D, Robotham B, Fell CJ, Jones D, Scully AD. New barrier encapsulation and lifetime assessment of printed organic photovoltaic modules. Sol Energy Mater Sol Cells. 2016; 155: 108-116.
21. Banerjee DA, Kessman AJ, Cairns DR, Sierros KA. Tribology of silica nanoparticle-reinforced, hydrophobic sol-gel composite coatings. Surf Coatings Technol. 2014; 260: 214-219.
22. Abu-Dheir N, Rifai A, Yilbas BS, Yousaf MR, Al-Sharafi A, Ali H, et al. Sol-gel coating of colloidal particles deposited glass surface pertinent to self-cleaning applications. Prog Org Coat. 2019; 127: 202-210.
23. Xu T, Yu L. How to design low bandgap polymers for highly efficient organic solar cells. Mater Today. 2014; 17: 11-15.
24. Lin W, Zheng J, Yan L, Zhang X. Sol-gel preparation of self-cleaning SiO_2-TiO_2/SiO_2-TiO_2 double-layer antireflective coating for solar glass. Results Phys. 2018; 8: 532-536.
25. Dou W, Wang P, Zhang D, Yu J. An efficient way to prepare hydrophobic antireflective SiO_2 film by sol-gel method. Mater Lett. 2016; 167: 69-72.
26. Wei G, Yang D, Zhang T, Yue X, Qiu F. Fabrication of multifunctional coating with high luminous transmittance, self-cleaning and radiative cooling performances for energy-efficient windows. Sol Energy Mater Sol Cells. 2019; 202: 110125.
27. Reese MO, Gevorgyan SA, Jørgensen M, Bundgaard E, Kurtz SR, Ginley DS, et al. Consensus stability testing protocols for organic photovoltaic materials and devices. Sol Energy Mater Sol Cells. 2011; 95: 1253-1267.
28. Roesch R, Faber T, Von Hauff E, Brown TM, Lira-Cantu M, Hoppe H. Procedures and practices for evaluating thin-film solar cell stability. Adv Energy Mater. 2015; 5: 1501407.
29. Davis RL, Jayaraman S, Chaikin PM, Register RA. Creating controlled thickness gradients in polymer thin films via flowcoating. Langmuir. 2014; 30: 5637-5644.
30. Bake A, Merah N, Matin A, Gondal M, Qahtan T, Abu-Dheir N. Preparation of transparent and robust superhydrophobic surfaces for self-cleaning applications. Prog Org Coatings. 2018; 122: 170-179.
31. Zhang Y, Samuel IDW, Wang T, Lidzey DG. Current status of outdoor lifetime testing of organic photovoltaics. Adv Sci. 2018; 5: 1800434.
32. Katz EA, Mescheloff A, Visoly-Fisher I, Galagan Y. Light intensity dependence of External Quantum Efficiency of fresh and degraded organic photovoltaics. Sol Energy Mater Sol Cells. 2016; 144: 273-280.
33. Karmalawi AM, Rayan DA, Rashad MM. Establishment and evaluation of photovoltaic quantum efficiency system at central metallurgical research and development institute. Optik. 2020; 217: 164931.

Enjoy *JEPT* by:

1. Submitting a manuscript
2. Joining in volunteer reviewer bank
3. Joining Editorial Board
4. Guest editing a special issue

For more details, please visit:
http://www.lidsen.com/journal/jept